Explanation for the $\sqrt{E}$-dependent mobilities of charge transport in molecularly doped polymers

David H. Dunlap
Department of Physics and Astronomy, University of New Mexico, Albuquerque, New Mexico 87131
(Received 29 December 1994; revised manuscript received 20 March 1995)

Although disorder is widely believed to be the primary distinguishing feature governing the transport of photoinjected charges in molecularly doped polymers, disorder theory has yet to convincingly explain why the linearity of the log of the mobility with the square root of the applied field persists over such a wide range. In this article a theory for high-field hopping transport in strongly disordered materials is developed which combines the elements of a continuous time random walk with existing variable-range hopping techniques. A self-consistent integral equation is derived from which the distribution of site energies for those sites which characterize the percolation pathways is determined. The theory is applied to an energetically disordered system and the mobility is calculated for the Miller-Abrahams form of the jump rate. It is shown that if the site energies belong to a Gaussian distribution, the logarithm of the mobility rises nearly linearly with $\sqrt{E}$ for electric fields spanning almost two decades. The slope is temperature dependent, and agrees with the Poole-Frenkel law.

I. INTRODUCTION

In time-of-flight experiments carried out in 1970, Pai[1] observed that the mobility of photo-injected holes in poly (N-vinylcarbazole) at high electric fields may be described by the Poole-Frenkel law,[2]

$$\mu=\mu_0 \exp\left[\frac{-\Delta}{kT}\right]\exp[\gamma\sqrt{E}\,]\,. \tag{1.1}$$

In expression (1.1), the mobility μ varies from 10^{-8} to 10^{-6} cm^2/V s, and the activation energy Δ is 0.5 eV. The behavior described by (1.1) has subsequently been observed for a variety of molecularly doped, pendant-, and main-chain polymers, as well as for vapor-deposited molecular glasses,[3] and its applicability has been demonstrated for electric field strengths E, ranging in some samples from 10^4 to 10^6 V/cm. It was shown by Gill[4] that the Poole-Frenkel factor γ is a function of temperature and is described empirically by

$$\gamma=B\left[\frac{1}{kT}-\frac{1}{kT_0}\right], \tag{1.2}$$

with $B\approx 4\times10^{-4}$ $(e^2\,\mathrm{V\,cm})^{1/2}$, and $T_0\approx 500$ K. Among experiments on a variety of host polymers and dopants, these parameters vary by no more than a factor of 2. In recent years, improvements in experimental sensitivity and in data analysis have exposed small deviations[5] from (1.2). But for a few exceptions,[6] there has been essentially no observed deviation in the gross dependence of $\log(\mu)$ on the $\sqrt{E}$ for changes in electric field of between two and three orders of magnitude.[7]

The molecularly doped polymers are ideal systems for the investigation of the underlying transport mechanisms because, in addition to field and temperature dependencies, the mobility may be studied as a function of dopant concentration. It has been demonstrated that the parameters μ_0, Δ, B, and T_0 are each functions of the average dopant separation ρ for variations in dopant concentration from between 10 and 90 %, i.e., for 10 Å $<\rho<$ 20 Å.[8] For example, the factor B increases by between 10 and 50 % with a doubling of ρ, and T_0 decreases by about the same percentage. In general, when the dopant molecules have a dipole moment less than $2D$, Δ increases with increasing ρ.[3] In N,N'-diphenyl-N,N'-bis(3-methylphenyl)-[1,1'-biphenyl]-4,4'-diamine (TPD)-doped bisphenol A polycarbonate, Δ increases from 0.2 to 0.5 eV as ρ increases from 8 to 17 Å.[8] On the other hand, for materials comprised of dopant molecules with dipole moments greater than 2.5 D, Δ is on the order of 0.5 eV, independent of concentration.[3,8] In cases where Δ is independent of concentration, the prefactor μ_0 decreases exponentially with ρ such that,

$$\mu_0=a_0\rho^2 e^{-2\rho/\rho_0}\,, \tag{1.3}$$

where $\rho_0\approx 1.5$ Å has been interpreted as the radius of a localized state associated with a dopant molecule. This behavior, together with the fact that the mobilities are rather low, suggests that transport takes place when charges hop from one dopant molecule to the next.

Except for the compensation factor $(1/kT_0)$, expressions (1.1) and (1.2) describe the Arrhenius dependence of the mobility which arises if moving charges must hop over a Coulomb barrier of height Δ in energy. In such a case, an electric-field dependence arises because the barrier height is lowered in a dc electric field by an amount $B\sqrt{E}$. For a dielectric constant κ of 3, the factor B is $(e^3/\pi\kappa\varepsilon_0)^{1/2}=4\times10^{-4}$ $(e^2\,\mathrm{V\,cm})^{1/2}$. This is, in fact, the value typically found in experiments. Thus the standard Poole-Frenkel model[2] gives, at first glance, a plausible explanation for the observed behaviors of these materials. Further inspection, however, reveals several inconsistencies. In particular, for typical field strengths of 10^5 V/cm the peak of the Coulomb barrier is at a separation distance of 63 Å, which is much larger than the mean dopant separation.[7] On the other hand, alternate at-

tempts to explain (1.1) and (1.2) have been shown to fail to quantitatively describe the experiment.[7,9–12] It has proved difficult to explain why the $\sqrt{E}$ dependence should be followed so precisely over so many decades if the basic physical principal is indeed different from the Poole-Frenkel mechanism. It is especially puzzling that there is such a steep rise of the mobility with field for field strengths $\lesssim 10^5$ V/cm, for in this case, the energy required to move an electron from one dopant to the next in the direction of the field, $e\rho E$, is but a fraction of kT.

Although an understanding of the $\sqrt{E}$ dependence in the molecularly doped polymers has proved somewhat evasive, other experimental observations have been explained by the application of hopping transport theories in disordered media. From the time-of-flight (TOF) curves of current I vs time t it was shown that transport in these materials is anomalously dispersive, in the sense that the ratio of the width w of the carrier packet to its mean position l is independent of time.[10] For normal (Gaussian) diffusion, in contrast, the ratio $w/l \sim t^{-1/2}$. In these systems apparently either w increases more quickly or l increases more slowly with time. In 1975, Scher and Montroll argued that such behavior in a random walk occurs when the distribution of dwell times $\Psi(t)$ has a divergent first moment.[13] This might be the case when small fluctuations in the interdopant spacing cause exponentially large fluctuations in the hopping rates. Specifically, Scher and Montroll showed that when

$$\Psi(t) \sim \frac{\alpha}{t^{1+\alpha}}, \tag{1.4}$$

where the disorder parameter α is between 0 and 1, the TOF current vs time curves display a property known as universality; all experimental data fall on the same curve when the scaled current $I(t)/I(\tau)$ versus the scaled time t/τ is displayed on a plot of $\log I$ vs $\log t$. (The time τ is a characteristic transit time which may be identified from the shoulder of a $\log I$-$\log t$ plot.) The current is described well by a power law, $I(t) \sim t^{-(1-\alpha)}$, before the shoulder, and by the steeper power law, $I(t) \sim t^{-(1+\alpha)}$, after the shoulder.

Following the success of the Scher-Montroll (SM) theory in describing the relationship between current and time, inquiries were made as to whether the same model might also be capable of explaining the ubiquitous $\sqrt{E}$ dependence of the mobility. Such an attempt to describe experimental data with the SM theory was made in 1977 by Pfister,[9] who argued that the hole mobilities in triphenylamine (TPA)-doped polycarbonate could be described by the expression

$$\mu = \nu_0 \frac{L}{E} \left[l_0/L \sinh \frac{e\rho E}{2kT} \right]^{1/\alpha} \exp\left[\frac{-\Delta}{kT} \right] . \tag{1.5}$$

In (1.5), ν_0 is an attempt frequency, L is the length of the sample, and $l_0 \sinh e\rho E/2kT$ is to be loosely interpreted as the mean distance traveled in the direction of the electric field in a single hop. Equation (1.5) follows directly from the SM formalism if it is assumed that the hopping rates are suppressed by the Arrhenius factor $\exp(-\Delta/kT)$, and also if the hopping rates in the direction of the field are enhanced by the factor $\exp(e\rho E/2kT)$, while those against the field are suppressed by the inverse factor, $\exp(-e\rho E/2kT)$. For consistency with the experimental data it was argued by Pfister that the exponent α should increase with temperature. Such a temperature-dependent α would arise if the origin for the broad distribution of pausing times were a variation in dopant energy levels. Indeed, the $\log I$ vs $\log t$ curves lend support to this notion. An increase of T is accompanied by a decrease in dispersion, which in turn corresponds to an increase of α. Another attempt to describe the electric-field dependence of the mobility in terms of the SM theory was made by Crisa in 1983.[14] For an oxadiazole doped polymer layer it was shown that the current-time curves are well characterized by the SM theory with a value of $\alpha = 0.80$. For high enough temperatures, the hyperbolic sine in (1.5) may be replaced by its argument, $e\rho E/2kT$. In such a case, the SM theory predicts that

$$\log\mu \cong \left[\frac{1}{\alpha} - 1 \right] \log \frac{E}{L} . \tag{1.6}$$

For the same value $\alpha = 0.80$, Crisa fit the electric field dependence and the length dependence of the mobility in oxadiazole with the function (1.6) for the range $E = 5\times10^4$ to 47×10^4 V/cm and $L = 5$ to 30 μm. Again it was noted that the temperature dependence of the slope of $\log\mu$ versus $\log E$ and the temperature dependence of the current-time curves are correlated in a consistent manner if it is assumed that α is an increasing function of temperature.

Improvements in the preparation of thin polymer films, and in experimental techniques for measuring TOF signals, have allowed for experiments with fewer carriers and a wider range of electric fields. Accompanying these improvements have been several changes in the basic experimental observations which have served to cast doubt on the applicability of the SM theory. As an early example, in contrast to the results of Pfister, investigations of TPA-doped polycarbonate by Borsenberger, Mey, and Chowdry[15] showed that the SM theory did not apply. The current before the shoulder in the I vs t curves tends to be flat rather than decaying. Yet, after the shoulder, the current retains an anomalously broad tail. At best, on a $\log I$-$\log t$ plot, data might be fit by defining two distinct disorder parameters, α_1 and α_2, where α_1 describes the decay of the current with time before the shoulder, and α_2 describes the width of the carrier distribution as determined from the current profile after the shoulder. Most of the recent current-time curves are not well described with two disorder parameters, however.[16] Scott, Pautmeier, and Schein[5] have shown that the shape of the current vs time curve after the shoulder is best described by a Gaussian distribution of effective carrier velocities. Furthermore, in contrast to the reported results of Crisa, the mobility does not scale with the sample width L, again suggesting that the theory of SM is inappropriate.[17] In spite of these experimental differences, one characteristic remains invariant; the log of the mobility remains proportional $\sqrt{E}$ for a wide class of materials, and over a wide range of field. For DEH(hydrazone)-doped bisphenol-A-polycarbonate the linearity with the $\sqrt{E}$ is

maintained for the field range $E=0.82\times10^4$ to 2.1×10^6 V/cm.[7]

The thesis of Pfister and of Crisa was that both the anomalously dispersive TOF profiles and the field-dependent mobilities in these experiments are a consequence of transport in a disordered medium. To further test these concepts while avoiding the uncontrolled approximations inherent in the Scher-Montroll theory, a study of disordered transport based on Monte Carlo simulations of a random walk has been carried out.[18–21] This approach has had reasonable success in predicting many of the general features of the mobility observed in these experiments. For example, the Monte Carlo simulation yields log$I$-log$t$ profiles which strongly resemble experiment. The $\sqrt{E}$ dependence of the log of the mobility has been shown to be consistent with simulations, albeit over a limited range in electric field.[21] In addition, in some systems, the mobility has been shown to decrease as a function of increasing field at lower fields, and the simulations also show such an initial decrease. Effective-medium theories of transport in disordered systems have been developed which lend support to the simulations.[22–25] None of the analytic forms, however, give rise to (1.1) or (1.2) over the broad range of electric fields observed in experiment.

In this article a theoretical description of disordered transport in molecularly doped polymers is developed which combines the elements of a continuous time random walk with the variable-range hopping theory of Apsley and Hughes,[26] and results ultimately in analytic expressions for anomalous transport which follow those of Scher and Montroll.[13] It will be shown that for reasonable parameters, the dependence of the log of the mobility on the $\sqrt{E}$ closely follows the Gill form for at least two decades of field. An outline of the remainder of this article is as follows. In Sec. II we describe the elements of a continuous time random walk. In doing so we develop an expression for the distribution of nearest-neighbor hopping rates which is based on the approach of Ref. 26. In Sec. III we show how the marginal distributions of hopping energies, direction cosines, and dwell times may be determined from the distribution of nearest-neighbor rates. We develop a general expression for the mobility as measured in a TOF experiment in Sec. IV. In Sec. V we develop analytic expressions for the case of energetic disorder only, when the hopping rate is of the Miller and Abrahams form. In order to illustrate general features of the theory we first describe qualitatively the results which would be obtained for a uniform site energy distribution. We then extend our approach to consider the case of a Gaussian distribution of site energies. Assuming the validity of specific assumptions regarding relevant time scales, the theoretical predictions are in good agreement with experiment. We discuss approximations and extensions of the present approach in Sec. VI, and the article is summarized in Sec. VII.

II. ELEMENTS OF A RANDOM WALK IN A DISORDERED MATERIAL

In developing an analytic form for the mobility in a disordered material, it is useful to start from a description of a continuous time random walk. In order to properly scale the time to hop from one dopant molecule to the next, we must first choose the underlying microscopic hopping rates. In keeping with the extensive work of Bässler,[21] we will consider a hopping rate with an asymmetric detailed balance factor; we shall take the rate $R_{i,j}$ to hop from dopant molecule i to dopant molecule j, to be of the form

$$R_{i,j}=\nu_0 e^{(-2\chi r_{i,j})} e^{-\beta/2[(\varepsilon_j-\varepsilon_i)-|\varepsilon_j-\varepsilon_i|]} . \tag{2.1}$$

In (2.1) $r_{i,j}$ is the spatial separation between molecule i and molecule j, ε_j is the energy of the donor level at molecule j, ε_i is the energy of the donor level at molecule i, and β is the Boltzmann factor. The prefactor ν_0 may be interpreted as an attempt frequency. This hopping rate has the one-sided detailed balance as found in the rate derived by Miller and Abrahams[27] to describe impurity band conduction is semiconductors; hops upwards in energy ($\varepsilon_j>\varepsilon_i$) are suppressed by the Boltzmann factor, while those downwards in energy are temperature independent. Such a hopping rate between two states comes about when the (otherwise localized) electronic states of a statically disordered system are temporarily mixed by vibrational distortions. A physical explanation for the asymmetric detailed balance is that phonons can always be emitted so that energy may be conserved in a downwards hop, but the probability to absorb a phonon of frequency $\omega=(\varepsilon_j-\varepsilon_i)/\hbar$ and hop upwards in energy will be scaled by the probability that such a phonon is available, $\exp(-\beta\hbar\omega)$. We note in passing that a symmetric form of the detailed balance factor arises when a small-polaron hopping rate is assumed.[28] Although the symmetric form is easier to work with analytically, its applicability in these systems is questionable, for the bare transfer-matrix element J which is required to quantitatively describe the data in these experiments has been found in some studies to be an order of magnitude larger than the bandwidth of typical molecular solids.[29]

The form of the hopping rate as expressed by (2.1) suggests that fluctuations in the jump rates may be quite large for the molecularly doped polymers. For typical energy differences in the range 0 to 0.2 eV, the exponent $\beta(\varepsilon_j-\varepsilon_i)$ is between 0 and 8 at room temperature. With $\chi\approx0.7$ Å^{-1}, a 10 Å variation in separation distance implies that $2\chi r$ may vary by 12. Thus the exponent $\mathcal{R}$ which determines the hopping rate for hops upwards in energy,

$$\mathcal{R}_{i,j}=2\chi r_{i,j}+\beta(\varepsilon_j-\varepsilon_i) \tag{2.2}$$

may vary by 20, giving rise to fluctuations of up to nine orders of magnitude in the jump rates.

In describing a continuous time random walk in the manner in which it may be implemented in a Monte Carlo simulation, one must determine the dwell time, the time to reside at a site once a random walker has arrived. One must also select the site to which the random walker will hop next. These two quantities are intimately related. A typical three-step selection algorithm which might be implemented in a Monte Carlo simulation is as follows:[21]

(1) Calculate the rates $R_{i,j}$ for a cluster of N sites, enumerated by the index j, surrounding the presently occupied site i. The cluster should be large enough so that there is essentially no probability of hopping outside its boundaries.

(2) For each rate $R_{i,j}$, extract a dwell time t_j from the associated Poissonian distribution of dwell times,

$$\Psi(t)=R_{i,j}e^{-R_{i,j}t} . \tag{2.3}$$

(3) Choose, as the next site to be visited, the site j, for which the time t_j is smallest, and assign this time as the dwell time which characterizes the hop from site i to site j.

When the hopping rates are extremely disparate, the site which is visited next is very often the site for which the rate $R_{i,j}$ is the largest. In 1974, Apsley and Hughes[26] showed how this idea may be implemented analytically to characterize transport in a spatially and energetically disordered system. The exponent,

$$\mathcal{R}_{i,j}=2\chi r_{i,j}+\frac{\beta}{2}[(\varepsilon_i-\varepsilon_j)-|\varepsilon_i-\varepsilon_j|] , \tag{2.4}$$

which determines the rate between site i and site j is to be considered a hyperradius in an augmented $\mathbf{r}\otimes\varepsilon$ space. The rule that the random walker hops to the site for which the rate is largest is equivalent to the statement that the random walker hops to the site which is a nearest-neighbor in this augmented space. Under such a rule, occasionally a random walker will hop beyond sites which are near in $\mathbf{r}$ because they are more distant in ε. When distance may be sacrificed for energy in this manner the transport process is commonly referred to as variable-range hopping.[30]

III. DISTRIBUTIONS FOR DWELL TIMES, DISTANCES AND DIRECTIONS

It should be clear from the above discussion that each hop in the random walk corresponds to a decision as to which site constitutes a nearest neighbor in the augmented space at the hyperradius $\mathcal{R}$. The dwell time, distance, direction, etc., which are ultimately settled upon are to be chosen from the corresponding distributions of those quantities which are associated with nearest-neighbor jumps. Calculating these distributions is the basic difficulty in describing transport in a disordered system. The distribution of possible rates out of a particular site depends on the energy and location of that site, and also on the energies and locations of the surrounding sites. Because some of the surrounding sites may have been visited on previous hops, the distribution of nearest-neighbor quantities describing the jump from a particular location can only be calculated if one can account for the path which has been followed to arrive at that location in the first place.

Substantial simplification arises if one ignores the path dependence of the distribution function. That is, the distribution of nearest-neighbor hyperradii $\mathcal{R}$ might be well represented by the distribution of $\mathcal{R}$ which are obtained with back transfer and the overlap of environments shared by adjacent sites completely neglected. This is certainly the spirit in which Apsley and Hughes calculate a distribution of nearest-neighbor $\mathcal{R}$, an approximation which we will also make at this point. We may now proceed to calculate the distribution of nearest-neighbor $\mathcal{R}$ which may be sampled in a disordered system in the presence of an electric field. At high fields, the energy gained in hopping in the direction of the field is an important factor in determining which site will be nearest neighbor. For these experiments it should therefore be included in the calculation of the hyperradius $\mathcal{R}$. We will approximate the field energy $eEr\cos\theta$ by $eE\rho\cos\theta$, since the most dramatic fluctuations in the field energy are the result of changes in direction. Thus we take

$$\mathcal{R}=2\chi r+\frac{\beta}{2}[(\varepsilon_2-\varepsilon_1-eE\rho\cos\theta) -|\varepsilon_2-\varepsilon_1-eE\rho\cos\theta|] . \tag{3.1}$$

The probability that the space between a hyperradius of 0 and $\mathcal{R}$ contains no neighbors, given that the energy of the site from which we make a jump is ε_1, is

$$P_{\mathcal{R}}=\exp[-V(\mathcal{R};\varepsilon_1)] , \tag{3.2}$$

where

$$V(\mathcal{R};\varepsilon_1)=N\int_{\mathcal{R}}\int\int 2\pi r'^2 dr' \sin\theta' d\Theta' \eta(\varepsilon_2')d\varepsilon_2' \tag{3.3}$$

is a volume in augmented space which is bounded by a surface at the hyperradius $\mathcal{R}$, $N=1/\rho^3$ is the dopant number density, and $\eta(\varepsilon)$ is the site energy density. (The details involved in calculating this surface are presented in Ref. 26.) It follows that

$$P(r,\theta,\varepsilon_2;\varepsilon_1)=N\exp[-V(\mathcal{R};\varepsilon_1)]2\pi r^2\sin\theta\eta(\varepsilon_2) \tag{3.4}$$

is the joint distribution function for the probability that the site which is a nearest neighbor is at a radius r, angle θ, and energy ε_2, given that the energy at the site from which the hop was made was ε_1. In what follows we will refer to ε_1 as the initial energy, since it is the energy of the site from which the hop is initiated. Similarly, ε_2 is one of the possible final energies of the site to which a hop is made. Integrating (3.4) over r and ε_2 gives

$$\Theta(\theta;\varepsilon_1)=\int_{r,\theta}\int P(r,\theta,\varepsilon_2;\varepsilon_1)dr\,d\varepsilon_2 , \tag{3.5}$$

the probability density for finding the nearest-neighbor dopant at the angle θ, given ε_1. The average distance traveled in the direction of the field in a single hop,

$$l_1\cong\rho\langle\cos\theta\rangle=\rho\int d\theta\cos(\theta)\int d\varepsilon_1\Theta(\theta;\varepsilon_1)g(\varepsilon_1) \tag{3.6}$$

is obtained by integrating over all angles. In (3.6) we have specifically indicated that an additional integration must be performed over the distribution of initial energies $g(\varepsilon_1)$. Note also that we have again approximated $\langle r\cos\theta\rangle$ by $\rho\langle\cos\theta\rangle$ in calculating l_1. The distribution of dwell times,

$$\psi(t;\varepsilon_1)=\int_0^\infty d\mathcal{R}\exp[-V(\mathcal{R};\varepsilon_1)]V'(\mathcal{R};\varepsilon_1) \times\nu_0\exp(-\mathcal{R}-\nu_0e^{-\mathcal{R}}t) , \tag{3.7}$$

is obtained by weighting the Poissonian corresponding to

each value of $\mathcal{R}$ by the probability that $\mathcal{R}$ is a nearest-neighbor distance. Finally, the distribution of site energies visited in the random walk $g(\varepsilon_1)$ can be determined via an iterative procedure. The probability density that a site with energy ε_2 will be hopped to, given that the initial site has energy ε_1,

$$P(\varepsilon_2;\varepsilon_1)=\int\int P(r,\theta,\varepsilon_2;\varepsilon_1)dr\,d\theta \tag{3.8}$$

is obtained by integrating (3.4) over r and θ. If we average $P(\varepsilon_2;\varepsilon_1)$ over all initial energies ε_1 which may be obtained along the random walk, we should obtain the distribution of final energies ε_2. Because each final energy becomes the initial energy for the subsequent hop, it follows that the distribution $g(\varepsilon)$ must satisfy the self-consistency condition

$$g(\varepsilon_2)=\int d\varepsilon_1 P(\varepsilon_2;\varepsilon_1)g(\varepsilon_1)\ . \tag{3.9}$$

The function $g(\varepsilon)$ which satisfies (3.9) may be obtained by iteration.

IV. CALCULATION OF THE MOBILITY FOR A TIME-OF-FLIGHT EXPERIMENT

In a time-of-flight experiment, a localized packet of electron-hole pairs is produced by illuminating a light-sensitive coating on one side of a polymer film which forms the weak link in a closed circuit. When a voltage is applied the electrons are quickly taken up by the anode. However, to reach the cathode, the holes must traverse the film. Their progress is monitored by measuring the current in the circuit as a function of time. When the holes reach the cathode the current begins to decrease noticeably, which allows for the determination of a transit time τ.[3] The drift velocity v is the ratio of the film thickness L to the transit time τ,[31]

$$v=\frac{L}{\tau}\ . \tag{4.1}$$

At the transit time, the centroid of the carrier packet will have moved a distance L. In terms of the quantities discussed in Sec. III, this implies that

$$L=l_1p_1(\tau)+l_2p_2(\tau)+l_3p_3(\tau)+\cdots=\sum_{n=1}^{\infty}l_np_n(\tau)\ , \tag{4.2}$$

where l_n is the average distance traveled in the direction of the applied field by a carrier which has hopped n times, and $p_n(\tau)$ is the probability that a carrier has hopped exactly n times in the time τ. With a few simplifications, the summation indicated in (4.2) may be performed. First, by the central limit theorem, for large n,

$$l_n\sim nl_1\ . \tag{4.3}$$

Second, the probabilities $p_n(\tau)$ may be determined from the distribution of dwell times:

$$p_n(\tau)=\int_0^{\tau}dt\psi_n(t)\left[1-\int_0^{\tau-t}dt'\psi(t')\right]\ , \tag{4.4}$$

where $\psi_n(t)$ is the n-fold convolution of the distribution of dwell times,

$$\psi_n=\psi\otimes\psi\otimes\psi\otimes\psi\cdots\ . \tag{4.5}$$

That there is a product of two terms in the integrand of (4.4) is easy to understand; the probability of hopping n times in a time between t and $t+dt$ is given by the first, while the second is the probability of not making yet another hop between the time t and the transit time τ. The distances l_n and the probabilities $p_n(\tau)$ are correlated because they are both influenced by the electric field. For example, when a hop is in the direction of the field, the dwell time, which is also a function of the field, will be smaller. In writing (4.2) we are ignoring this correlation. It can be shown that this is justified in keeping with the fact that for large enough n, those carriers experiencing n hops will have moved essentially the same distance. Each function $\psi(t)$ in the convolution in (4.5) depends on an energy which is drawn from the distribution of visited site energies $g(\varepsilon)$. Therefore, to calculate $\psi_n(t)$, we must properly average over all possible sequences of energies. This is best carried out in the Laplace domain.

For a particular sequence of energies, the Laplace transform of the distribution of time to perform n hops is,

$$\tilde{\psi}_n(s;\varepsilon_1,\varepsilon_2,\varepsilon_3\cdots\varepsilon_n)=\prod_{i=1}^{n}\tilde{\psi}(s;\varepsilon_i)\ . \tag{4.6}$$

In (4.6) $\tilde{\psi}_n(s)$ denotes the Laplace transform of $\psi_n(t)$, where s is the Laplace variable. Taking the log of both sides of (4.6), we see that for large n, the log of $\tilde{\psi}_n(s)$ approaches n times the configurational average of the log of $\tilde{\psi}_n(s)$:

$$\ln[\tilde{\psi}_n(s;\varepsilon_1,\varepsilon_2,\varepsilon_3\cdots\varepsilon_n)]=\sum_{i=1}^{n}\ln[\tilde{\psi}(s;\varepsilon_i)]\sim n\langle\ln[\tilde{\psi}(s;\varepsilon)]\rangle\ , \tag{4.7}$$

where the angle brackets denote an integration over the distribution $g(\varepsilon)$. Therefore, we substitute for (4.6) the asymptotic form,

$$\tilde{\psi}_n(s)\sim\exp\{n\langle\ln[\tilde{\psi}(s;\varepsilon)]\rangle\}\ . \tag{4.8}$$

Combining (4.8), (4.3), and (4.2), we obtain the following expression for the width of the film as a function of the transit time:

$$\begin{aligned}L&=l_1\int_{\gamma-i\infty}^{\gamma+i\infty}ds\,e^{s\tau}\frac{1-\langle\tilde{\psi}(s)\rangle}{s}\sum_{n=1}^{\infty}n\exp\{n\langle\ln[\tilde{\psi}(s)]\rangle\}\\&=l_1\int_{\gamma-i\infty}^{\gamma+i\infty}ds\,e^{s\tau}\frac{\{1-\langle\tilde{\psi}(s)\rangle\}\exp\{\langle\ln[\tilde{\psi}(s)]\rangle\}}{s(1-\exp\{\langle\ln[\tilde{\psi}(s)]\rangle\})^2}\ .\end{aligned} \tag{4.9}$$

The integrals in (4.9) follow the Abromwich contour for Laplace inversion. To calculate the mobility, we first solve (4.9) for $\tau(L)$. The mobility is then, by definition,

$$\mu=\frac{L}{E\tau(L)}\ . \tag{4.10}$$

The reader will recognize that Eqs. (4.9) and (4.10) are

formally equivalent to the results of Scher and Montroll.[13] For example, the Laplace inverse of $\exp\{\langle \ln[\tilde{\psi}(s;\varepsilon)]\rangle\}$ may be identified with the Scher-Montroll pausing-time distribution function $\Psi(t)$. There are several characteristics which are specific to a disorder model which are brought out in the present approach. First, the pausing time distribution function is defined as the distribution of times which correspond to various *nearest-neighbor* jump rates which may be encountered at different locations in the sample. Second, the average distance traveled in the direction of the field per hop l_1, which depends both on the electric field and the disorder, is defined explicitly by expression (3.6). And third, for the case of energetic disorder, the present approach addresses the question of assigning an initial energy ε_1 for each successive hop, via an iterative solution of (3.9).

V. APPLICATIONS

In this section we will calculate the mobility for the specific case in which the only disorder is due to site energy differences arising from the nonhomogeneous environment; to a large extent, we will neglect the effects of spatial disorder. In light of the discussion in Sec. II, the neglect of spatial disorder appears to be absurd at first glance. After all, extremely large fluctuations in jump rates may be attributed to small spatial fluctuations in dopant separation,[13] and it is the tremendous disparity among the various hopping rates which suggests that the conducting pathways may be characterized by the largest of the rates, i.e., the rates of defining nearest-neighbor jumps. We should make it clear in advance, therefore, that we will neglect the details of the spatial disorder in what follows partly for calculational efficiency; the approximation we make below is to treat the variable r, which describes the separation between dopant molecules, as a constant. In practice, the numerical integrations which must be performed to reduce the joint distribution function $P(r,\theta,\varepsilon_2;\varepsilon_1)$ to its marginals are time consuming; we substantially speed up the computation by eliminating the integration over r. In addition to this practical advantage, however, we are driven to the constant-r approximation by the experimental findings of a temperature-dependent disorder parameter α. We will see that the temperature dependence of α arises from the energetic disorder, and that the essence of this temperature dependence is most clearly exhibited when the radial fluctuations are suppressed.

In holding the variable r constant, we describe a contrived model in which all of the neighboring dopants have the same separation. We will assume that each dopant molecule is connected to M spatial nearest neighbors, where M is 12, the coordination number for a hexagonal close-packed structure. We take the dopant separation to be a constant, $\rho=9$ Å, but we retain the angular component of the energy fluctuation which is due to the electric field. The interpretation is that the M neighbors under consideration are at random locations on the surface of a sphere of radius ρ. We ignore excluded volume effects. The present section is divided into two distinct subsections: Case (i) is an examination of the mobility when the site energy distribution is uniform, and case (ii) is a repeat of case (i), but for a Gaussian site energy distribution.

Case (i): Uniform site energy distribution

In order to illustrate general features of the calculation, we begin by considering a uniform distribution of site energies with full width W,

$$\eta(\varepsilon)=\frac{1}{W};\quad 0\le\varepsilon<W\ . \tag{5.1}$$

We take $W=0.7$ eV. In this case, the joint distribution function for the probability that the site which is a nearest neighbor is at an angle θ and energy ε_2 is

$$P(\theta,\varepsilon_2;\varepsilon_1)=\begin{cases}\left[1-\left[1-\dfrac{A_1(\varepsilon_1)}{2W}\right]^M\right]\times\dfrac{1}{A_1(\varepsilon_1)}; & \varepsilon_2-eE\rho\cos\theta-\varepsilon_1<0\\ \left[1-\dfrac{A_1(\varepsilon_1)}{2W}\right]^M\times\left[1-\dfrac{A_2(\varepsilon_2,\theta;\varepsilon_1)}{2W-A_1(\varepsilon_1)}\right]^{M-1}\dfrac{M}{2W-A_1(\varepsilon_1)}; & \varepsilon_2-eE\rho\cos\theta-\varepsilon_1\ge 0\ .\end{cases} \tag{5.2}$$

In (5.2), $A_1(\varepsilon_1)$ and $A_2(\varepsilon_2,\theta;\varepsilon_1)$ are areas on a two-dimensional $\{\varepsilon_2,\cos\theta\}$ plane, as illustrated in Fig. 1. That the expression (5.2) is defined separately for two different regions may be understood as follows: For all sites for which $\varepsilon_2-eE\rho\cos\theta-\varepsilon_1<0$ the hopping rates are equivalent, and therefore the distribution in θ and ε_2 is flat: On the other hand, for the sites for which $\varepsilon_2-eE\rho\cos\theta-\varepsilon_1\ge 0$, the hopping rates are extremely disparate, and the distribution is of the form of Eq. (3.4). The first factor on the bottom (top) right-hand side of (5.2) gives the probability that none (at least one) of the M neighbors has energy and angle such that $\varepsilon_2-eE\rho\cos\theta-\varepsilon_1$ is less than zero. The reason for this all-or-nothing state of affairs is that if for *just one* of the neighbors, $\varepsilon_2-eE\rho\cos\theta-\varepsilon_1$ is less than zero, the hop will surely be to that site (rather than to a site for which $\varepsilon_2-eE\rho\cos\theta-\varepsilon_1>0$) and hence ε_2 and $\cos\theta$ should be chosen from a uniform distribution.

To further clarify (5.2), we should remark that the Miller-Abrahams form of the hopping rate has forced us to break away from considering *only* the hopping rates to the nearest neighbors in an augmented space; the hopping rates for all sites for which $\varepsilon_2-eE\rho\cos\theta-\varepsilon_1<0$ clearly do not obey the criteria of being extremely disparate. In such a case, one would normally choose the next site by a consideration of the associated Poissonian

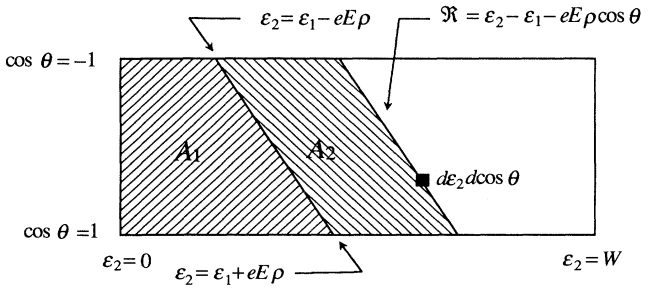

FIG. 1. Shown, for a particular value of the initial energy ε_1, is the two-dimensional energy-angle phase plane from which is determined the distribution of hopping directions and energies. The abscissa indicates the (final) site energy ε_2, which may lie anywhere between 0 and W for the case of a uniform distribution, and the ordinate indicates the direction cosine (with respect to the applied field) for the hop. Hence, the total area in the phase plane is $2W$. The plane is divided into two distinct regions, above and below the line $\varepsilon_2-\varepsilon_1-eE\rho\cos\theta=0$. If the coordinates (ε_2,θ) for a neighboring site fall to the left of the line, then the hopping rate (to that particular site) is ν_0; if they fall to the right, the hopping rate is $\nu_0\exp[-\beta(\varepsilon_2-\varepsilon_1-eE\rho\cos\theta)]$. The ratio, $A_1/2W$, is the probability that the coordinates of a neighboring site are to the left of the line; the probability that the coordinates for *all* M of the neighboring sites will be found to the right of the line is $(1-A_1/2W)^M$, etc. The probability to hop to a site with energy ε_2 at an angle θ with respect to the applied electric field is given by the product of the area $d\varepsilon_2 d\cos\theta$, represented in the figure by the black square, and the appropriate scale factor given in expression (5.2). The area A_2 is defined by the area between the line $\varepsilon_2-\varepsilon_1-eE\rho\cos\theta=0$ and a parallel line passing through the point $(\varepsilon_2,\cos\theta)$.

distributions of dwell times, as described in Sec. II. Such a procedure is not necessary here, however, for the simple fact that the rates are *equivalent* when $\varepsilon_2-eE\rho\cos\theta-\varepsilon_1<0$. Consequently, as the energy difference $\varepsilon_2-eE\rho\cos\theta-\varepsilon_1$ goes from positive to negative, the distribution of nearest neighbors goes from the multidimensional Poissonian described by (3.4), to a uniform distribution.

Numerically integrating (5.2) over the angle θ gives $P(\varepsilon_2;\varepsilon_1)$ for various strengths of the electric field. With this conditional distribution, (3.9) is iterated to obtain the distribution of site energies $g(\varepsilon)$ which are visited on the random walk. For the initial guess $g(\varepsilon)=\delta(\varepsilon)$, the iterative procedure converges rapidly; for all ε the relative difference in $g(\varepsilon)$ between successive iterations is less than 1% after about ten iterations. The number of hops after which the system may be said to have equilibrated is therefore of the same order. Figure 2 shows the calculated function $g(\varepsilon)$ for several electric-field strengths. It is peaked at $\varepsilon=0$, and is relatively insensitive to the field for $E\lesssim 50$ V/μm. Because we are considering only energetic disorder, the Boltzmann factor scales out of expression (3.3) for the hypervolume. As a consequence, the distribution $g(\varepsilon)$ only depends on the relative weights in the two-dimensional phase space, and does not depend on temperature.

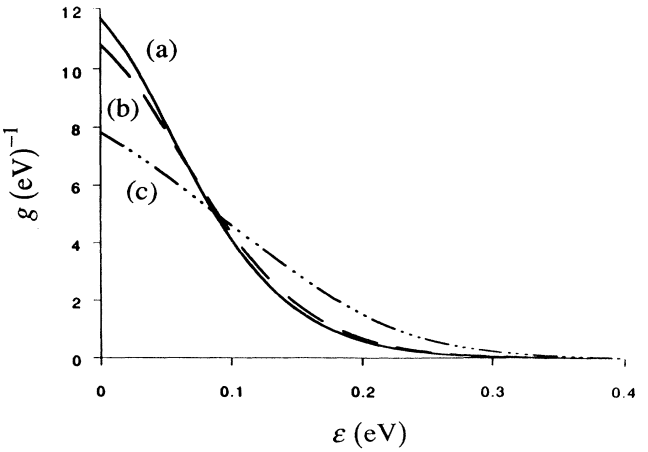

FIG. 2. The distribution of energies of those sites which are visited in the random walk $g(\varepsilon)$ is plotted versus ε for three electric-field strengths: (a) $E=1\times10^5$ V/cm, (b) $E=4\times10^5$ V/cm, and (c) $E=14\times10^5$ V/cm. The underlying site energy distribution is uniform, with width $W=0.7$ eV. We see that the energies of the sites which are visited are crowded to the bottom of the band, for $\varepsilon\lesssim0.1$ eV. As the electric field is increased, the distribution broadens, but the most probable value of ε remains at $\varepsilon=0$.

The average distance traveled in the direction of the field in a single hop is obtained by substituting the function $g(\varepsilon)$ into (3.6) and performing the angular integration. The relation between l_1 and E is displayed in Fig. 3. Note that l_1 increases linearly with E for the fields under consideration, except for the largest field strengths, where

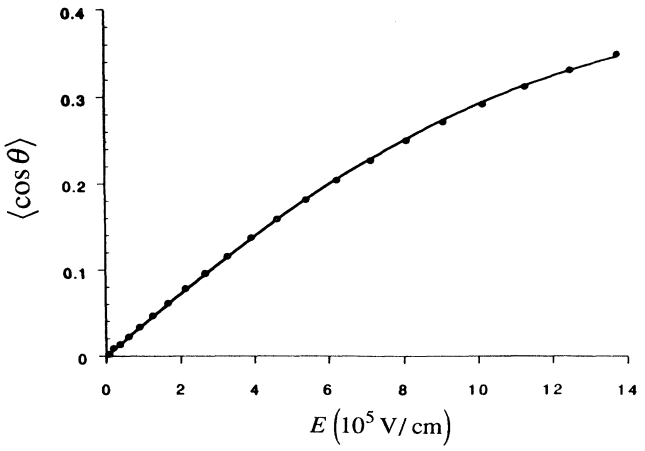

FIG. 3. The average distance hopped in the direction of the field is given by $l_1(E)=\rho\langle\cos\theta\rangle$. In this figure is shown the average projection of a hop in the direction of the electric field, $\langle\cos\theta\rangle$, as a function of the field. At low fields $\langle\cos\theta\rangle$ increases linearly with field. At high fields it begins to saturate. The points were calculated from the theory. The solid line is a best fit to the function $\langle\cos\theta\rangle=C_1\tanh(C_2eE\rho/W)$, for which the fit parameters $C_1=0.42$ and $C_2=6.7$ are functions of only M.

it begins to saturate. Since $g(\varepsilon)$ is independent of temperature, so is the function $l_1(E)$. For the range of fields in experiment, the l_1 vs E curves are well described by the empirical form,

$$l_1(E)=\rho C_1 \tanh(C_2 eE\rho/W) , \tag{5.3}$$

where the constants $C_i=C_i(M)$ may depend only on the coordination number. For the present case in which $M=12$, we find that $C_1=0.42$ and $C_2=6.7$. We should note that (5.3) differs substantially from the nonlinear form for $l_1(E)$ assumed by Pfister[9] [cf. Eq. (1.5)]. The only quantity which remains to be calculated to specify the relation between L and τ is the Laplace transform of the effective pausing-time distribution function, $\exp\{\langle \ln[\tilde{\psi}(s)]\rangle\}$. For behavior at long times we are interested in the functional dependence on the Laplace variable s in the limit where s tends to zero. To shed light on the expected results of this calculation in advance, we will digress at this point and examine the representative form of the pausing-time distribution function which arises when $g(\varepsilon)$ is replaced by $\delta(\varepsilon)$ and the electric field is neglected.

Replacing $g(\varepsilon)$ by $\delta(\varepsilon)$ to obtain the effective pausing-time distribution is a crude approximation, but not without some merit. Equation (4.6) indicates that the time for n hops across the sample is to be calculated by adding together n times which are drawn from the distribution $\psi(t)$. This is just an estimate of the average dwell time multiplied by the factor n. Let us suppose that $\psi(t)\sim 1/t^{1+\alpha}$. Then, for $\alpha\leq 1$ the first moment of $\psi(t)$ diverges, which leads to the result that the sum of n times does not scale as L, but rather as $L^{1/\alpha}$. It is this well-known feature which gives rise to the length-dependent mobilities and anomalous dispersion predicted by SM. As the number of hops required to traverse the sample becomes larger, the sum of times is increasingly dominated by the times for the slowest hops. These hops are necessarily uphill in energy, and are therefore those which have originated from ε near the bottom of the distribution. We choose to ignore the electric field in calculating $\psi(t)$ at long times because the slowest hops represent climbs over the highest energetic barriers, which are necessarily those barriers which are not appreciably lowered by the electric field. (In hindsight we will see that this is a reasonable approximation for the case of a uniform site energy distribution; a Gaussian site energy distribution is another matter, however.) In such a case, the distribution of hyperradii is given by the one-dimensional distribution,

$$P(\mathcal{R})=\left[1-\frac{\mathcal{R}}{\beta W}\right]^{M-1}\frac{M}{\beta W};\quad 0\leq\mathcal{R}<\beta W . \tag{5.4}$$

In comparison to an algebraically decaying distribution of dwell times, the factor $\nu_0\exp(-\mathcal{R})\exp(-\nu_0 e^{-\mathcal{R}}t)$ in the integrand of (3.7) is narrow, and may as well be replaced by a δ function,

$$\nu_0\exp(-\mathcal{R})\exp(-\nu_0 e^{-\mathcal{R}}t)\cong\nu_0\delta(\nu_0 t-e^{\mathcal{R}}) . \tag{5.5}$$

Substitution of (5.4) and (5.5) into (3.7) gives the approximate distribution of dwell times,

$$\psi(t)=\frac{M}{\beta W}\frac{1}{t}\exp[(M-1)\ln(1-\ln\nu_0 t/\beta W)] ;$$
$$1\leq\nu_0 t<e^{\beta W} . \tag{5.6}$$

Because the distribution of site energies is compact, the distribution $\psi(t)$ must eventually be bounded by a decaying exponential. Expression (5.6) is a valid approximation because in practice this bound is not realized. For a site energy difference of 0.5 eV, the dwell time will be on the order of one second (for $\nu_0\sim 10^{13}$ s^{-1}); in contrast, the time-of-flight in these systems is typically recorded in milliseconds. Thus, for times of interest, $\ln\nu_0 t\ll\beta W$.

Expanding the logarithm in the exponent of (5.6) to first order in $\ln(\nu_0 t)/\beta W$, we obtain an approximate expression for a normalized distribution of dwell times which is of the SM form,

$$\psi(t)\cong\frac{\alpha\nu_0}{(\nu_0 t)^{1+\alpha}};\quad 1\leq\nu_0 t<\infty , \tag{5.7}$$

where at 300 K the disorder parameter,

$$\alpha=\frac{M-1}{\beta W}=0.39 , \tag{5.8}$$

is less than 1. At this point, the algebra follows SM. For $\alpha<1$, the Laplace transform of (5.7),

$$\tilde{\psi}(s)=1-\Gamma(1-\alpha)(s/\nu_0)^{\alpha}+\sum_{m=0}^{\infty}(-1)^m\frac{(s/\nu_0)^{m+1}}{m+1-\alpha} . \tag{5.9}$$

As s approaches zero, the integrand of the right-hand side of (4.9) is, asymptotically,

$$\frac{1}{s(1-\tilde{\psi})}\sim\frac{1}{\nu_0\Gamma(1-\alpha)(s/\nu_0)^{1+\alpha}} . \tag{5.10}$$

Inverting (5.10) for long times, one obtains the asymptotic result,

$$L\sim l_1\frac{(\nu_0\tau)^{\alpha}}{\Gamma(1-\alpha)\Gamma(1+\alpha)} . \tag{5.11}$$

Solving (5.11) for τ in terms of L and substituting the result into (4.10), we obtain the mobility,

$$\mu=\nu_0\frac{L}{E}\left[\frac{\rho C_1\tanh(C_2 eE\rho/W)}{L\Gamma(1-\alpha)\Gamma(1+\alpha)}\right]^{1/\alpha} . \tag{5.12}$$

Taking the logarithm of (5.12) we see that

$$\ln\mu\sim\left[\frac{1}{\alpha}-1\right]\ln E+\text{const}$$
$$=\frac{W}{M-1}\left[\frac{1}{kT}-\frac{M-1}{W}\right]\ln E+\text{const} \tag{5.13}$$

in the range where $\tanh(C_2 eE\rho/W)\sim C_2 eE\rho/W$. Expanding the factor $\ln E$ in (5.13) about an intermediate value of the square root of the electric field, say $\sqrt{E_0}=600$ (V/cm)$^{1/2}$, we obtain

$$\ln\mu \cong \frac{2W}{\sqrt{E_0}(M-1)}\left[\frac{1}{kT}-\frac{M-1}{W}\right]\sqrt{E}+\text{const}. \tag{5.14}$$

Equation (5.14) is of the Gill form, from which we may deduce a proportionality constant

$$B=\frac{2W}{\sqrt{E_0}(M-1)}=2.1\times10^{-4}(e^2\,\text{V cm})^{1/2} \tag{5.15}$$

and a compensation temperature

$$T_0=\frac{W}{k(M-1)}=740\ \text{K}\ . \tag{5.16}$$

Equation (5.13) predicts a rise of the log of the experimentally determined mobility with the log of the electric field, and therefore does not describe the linearity with $\sqrt{E}$ which is observed over so many decades. Nevertheless, for reasonable choices of W and M we see that the local slope of $\ln\mu$ vs $\sqrt{E}$ is in good agreement with that which is observed in experiment, as are the extracted parameters B and T_0. Thus, (5.12) lends support to the ideas of Pfister and of Crisa—that there should be a close link between the electric-field dependence of the mobility and the dispersivity in the current vs time curves. Namely, we observed that the dispersion parameter

$$\alpha=\frac{2kT}{B\sqrt{E_0}} \tag{5.17}$$

is connected to the Poole-Frenkel factor, and should increase with increasing temperature. Having worked out this simplified example for its analytic value, let us return now to considerations of a general $g(\varepsilon)$.

It is straightforward to calculate the dependence of the integrand in (4.9) on the Laplace variable s. For convenience we first introduce the function $f(s)=1-\tilde{\psi}(s)$. For small s, $f(s)\ll1$, and

$$\langle\ln[\tilde{\psi}(s)]\rangle\sim-\langle f(s)\rangle\ . \tag{5.18}$$

Expanding the integrand on the right-hand side of Eq. (4.9) to lowest order in $\langle f(s)\rangle$, we see that $[1-\exp\{\langle\ln[\tilde{\psi}(s)]\rangle\}]^2\sim\langle f(s)\rangle^2$, so that (4.9) becomes,

$$L\sim l_1\int_{\gamma-i\infty}^{\gamma+i\infty}ds\,e^{s\tau}\frac{1}{s\langle f(s)\rangle}\ . \tag{5.19}$$

If we had true algebraic scaling of the SM type, we would find that for small s, $\langle f(s)\rangle\sim As^{\alpha}$. In this case, the function $\langle f(s)\rangle$ has been obtained for small s by integrating the joint distribution function $P(\theta,\varepsilon_2;\varepsilon_1)$ over θ,ε_2, and ε_1, weighted by $g(\varepsilon_1)$ and $1-\tilde{\psi}(s)$;

$$\langle f(s)\rangle=\int\int\int d\theta\,d\varepsilon_2 d\varepsilon_1 P(\theta,\varepsilon_2;\varepsilon_1)g(\varepsilon_1)\times\left\{\frac{s}{(s+\nu_0 e^{-\mathcal{R}})}\Omega(\varepsilon_2-eE\rho\cos\theta-\varepsilon_1)+\sum_{n=1}^{M}\frac{s}{(s+n\nu_0)}\binom{M}{n}\frac{(1-A_1/2W)^n(A_1/2W)^{M-n}}{1-(1-A_1/2W)^M}[1-\Omega(\varepsilon_2-eE\rho\cos\theta-\varepsilon_1)]\right\}. \tag{5.20}$$

The two terms in the integrand of (5.20) describe $1-\tilde{\psi}(s)$ for the regimes in which $\varepsilon_2-eE\rho\cos\theta-\varepsilon_1\geq0$ and $\varepsilon_2-eE\rho\cos\theta-\varepsilon_1<0$, respectively; Ω is the step function. For the latter, each entry in the sum over the index n weights $1-\tilde{\psi}(s)$ by the probability that n of the M surrounding sites are such that $\varepsilon_2-eE\rho\cos\theta-\varepsilon_1<0$. For small s/ν_0, however, only the first of the two terms in (5.20) makes a significant contribution to the integral, which means that the mobility is determined primarily by those hops which are upward in energy. The result of the integration of (5.20) is shown in Fig. 4, where $\log_{10}\langle f(s)\rangle$ is plotted as a function of $\log_{10}(s/\nu_0)$ for the case in which $M=12$, $W=0.7$ eV, and $T=300$ K. Although a strict power law of the SM type is not obeyed, for reasonably small values of s the slope is much smaller than 1. For example, when $s/\nu_0\sim10^{-6}$ we find a slope of 0.7, whereas for $s/\nu_0\sim10^{-2}$ the slope is 0.5 Scher and Montroll have suggested that, when the change in the logarithmic slope is slow enough with respect to time, as a working approximation, one might replace the actual pausing-time distribution by a power law with an effective α.[13] In our case, the effective α is the slope of the $\log\langle f(s)\rangle$ vs $\log s$ curve, evaluated at a value of s which is proportional to the inverse of the transit time.

The two curves in Fig. 4 were calculated for two different electric-field strengths, $E=1\times10^5$ V/cm, and $E=14\times10^5$ V/cm, respectively. Although the electric field does broaden the distribution of initial energies $g(\varepsilon_1)$, as we have seen in Fig. 3, apparently this broadening has only a minor effect on $\langle f(s)\rangle$. This is in part because the dominant contribution to $\langle f(s)\rangle$ in the average over ε_1 comes from the edge of the distribution, near $\varepsilon_1=0$; we see in Fig. 3 that the edge of the distribution is not shifted by the electric field. Another reason for the lack of field dependence, however, is that even at $E=14\times10^5$ V/cm, the energy $eE\rho\approx0.1$ eV is only a fraction of $W=0.7$ eV. Without a strong additional field dependence to $\langle f(s)\rangle$, the log of the mobility will noticeably follow $\log(E)$, rather than $\sqrt{E}$, at high fields. Although decreasing the width W increases the field dependence of $\langle f(s)\rangle$, at the same time it dramatically increases the departure of $\langle f(s)\rangle$ from a power law function of s. For this reason, at this point we will abandon further analysis of the uniform site energy distribution, and move on to consider the case of a Gaussian site energy distribution, for which these conditions are better satisfied.

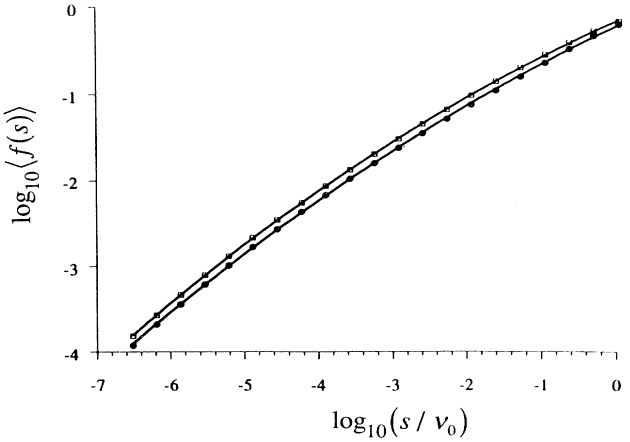

FIG. 4. Shown is $\log_{10}\langle f(s)\rangle$ as a function of $\log_{10}(s/\nu_0)$ for the case in which $M=12$, $W=0.7$ eV, and $T=300$ K. The points are calculated from (5.20); the smooth curves are empirical parabolic fits. The full width of the disorder W was taken to be 0.7 eV (large) so that the effective α, as calculated from the slope of the curve, might describe the anomalous transport regime ($\alpha<1$). The upper curve is for $E=1\times10^5$ V/cm, and the lower curve is for $E=14\times10^5$ V/cm. The small decrease of $\log_{10}\langle f(s)\rangle$ with field is a result of the field broadening of $g(\varepsilon_1)$. It is a small effect for two reasons: (a) as W becomes larger the field gradually has a smaller influence on the nearest-neighbor dwell time, and (b) the $\log_{10}\langle f(s)\rangle$ is determined by the location of the peak of $g(\varepsilon_1)$, which, for the case of a uniform density of states, does not shift with field.

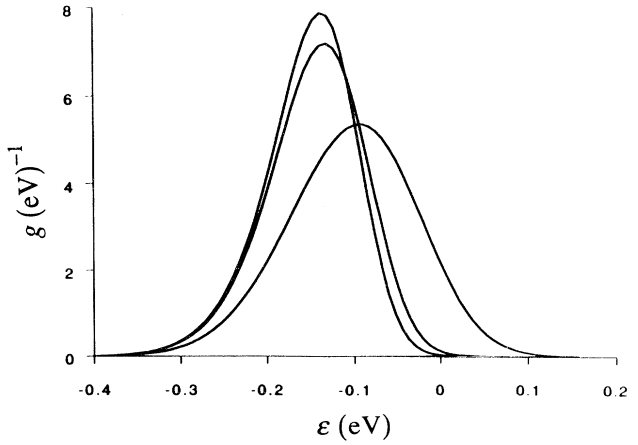

FIG. 5. The distribution $g(\varepsilon)$ is plotted versus ε for the case in which the site energy distribution is Gaussian, with $\sigma=0.1$ eV. From left to right, the peaks of the three curves shown correspond to the electric-field strengths $E=1\times10^5$ V/cm, $E=4\times10^5$ V/cm, and $E=14\times10^5$ V/cm, respectively.

Case (ii): Gaussian site energy distribution

The calculations above are easily repeated for nonuniform distributions of site energies. Here again following Bässler,[21] we will consider the case in which $\eta(\varepsilon)$ is a Gaussian, centered about $\varepsilon=0$ with a standard deviation $\sigma=0.1$ eV. We will again assume that $M=12$ and $\rho=9$ Å. For the initial guess that the distribution of starting energies $g(\varepsilon)=\delta(\varepsilon)$, the iteration of (3.9) converges quickly to a stationary distribution with a centroid at $\varepsilon\approx-2\sigma$. Figure 5 shows $g(\varepsilon)$ for three different values of the electric field; $E=1\times10^5$ V/cm, 4×10^5 V/cm, and 14×10^5 V/cm. As the electric field is increased, the left-hand shoulder of the distribution tends to remain fixed, while the right-hand shoulder moves to higher energies. In this manner the distribution tends to widen at high fields. In Fig. 6 is shown the function $l_1(E)$. The dependence on E is similar to that which we found in case (i) in that l_1 increases linearly for small E, but then begins to saturate for fields at the top of the range. Expression (5.3), with a substitution of σ for W, fits the field dependence of l_1 for the parameters $C_1=0.50$ and $C_2=1.0$. In Fig. 7 is shown the $\log\langle f(s)\rangle$ vs $\log s$ relation for $T=300$ K for two values of the electric field: $E=1\times10^5$ V/cm and $E=14\times10^5$ V/cm. For the same value of $\log s$, the slope is larger than in case (i), but this simply reflects the fact that the width of the distribution is smaller. Because the slope changes algebraically with $\log s$, we will assume that the concept of an effective disorder parameter α which scales with transit time is valid.

If we generate a $\log\langle f(s)\rangle$ vs $\log s$ curve at low field with a single value of ε_1, rather than averaging over the distribution $g(\varepsilon_1)$, we find good agreement with the curves in Fig. 7 when choosing $\varepsilon_1\cong-0.25$ eV. This suggests that at low electric field the hops which characterize the long-time behavior of the pausing-time distribution are typically originating from sites whose energies are 2.5 standard deviations lower than the mean site energy (and lower than the peak of $g(\varepsilon)$ by about $\sigma/2$). In contrast to case (i), there is a marked tendency for the electric field to lower the ordinate of the $\log\langle f(s)\rangle$ vs $\log s$ curve. On examining Fig. 7 we note that, for $s/\nu_0=10^{-3}$, when $E=14\times10^5$ V/cm, $\langle f(s)\rangle$ is smaller by a factor of 3 than it is when $E=1\times10^5$ V/cm. In Fig. 8 is shown $\log_{10}\langle f(s)\rangle$ as a function of E, for $s/\nu_0=10^{-3}$ at the two

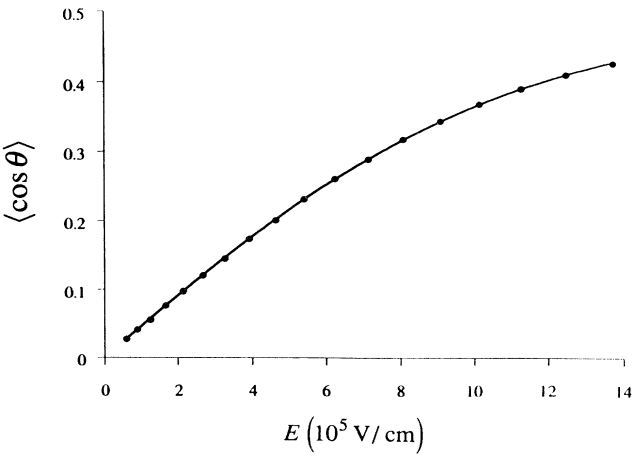

FIG. 6. The average projection of the hopping direction with respect to the electric field, $\langle\cos\theta\rangle$, is plotted as a function of the field, for the case in which the site energies are from a Gaussian distribution with $\sigma=0.1$ eV. The solid line is a best fit to the function $\langle\cos\theta\rangle=C_1\tanh(C_2eE\rho/\sigma)$, for which the parameters are $C_1=0.50$ and $C_2=1.00$.

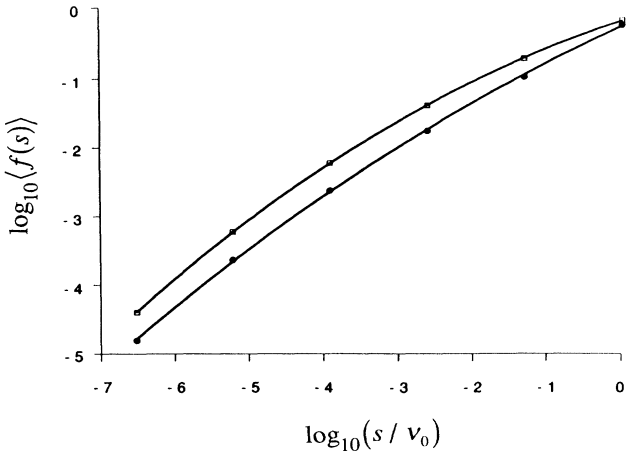

FIG. 7. For a Gaussian distribution of site energies, the $\log_{10}\langle f(s)\rangle$ is shown as a function of $\log_{10}(s/\nu_0)$, for the parameters $M=12$, $\sigma=0.1$ eV, and $T=300$ K. The points are calculated from (5.20); the smooth curves are empirical parabolic fits. The upper curve is for $E=1\times10^5$ V/cm, and the lower curve is for $E=14\times10^5$ V/cm, showing decrease in $\langle f(s)\rangle$ by about a factor of 3 over the range of field considered. In comparison, there is very little change in $\langle f(s)\rangle$ for fields smaller than $E=1\times10^5$ V/cm.

temperatures $T=300$ and 200 K. (The choice $s/\nu_0=10^{-3}$ has been made somewhat arbitrarily to correspond to a representative transit time which is still short enough to give rise to dispersive transport.) We have fit the curves to the empirical form,

$$\langle f(s)\rangle=\langle f_{E=0}(s)\rangle\exp[-C_3(eE\rho/\sigma)^{\xi}]\ , \tag{5.21}$$

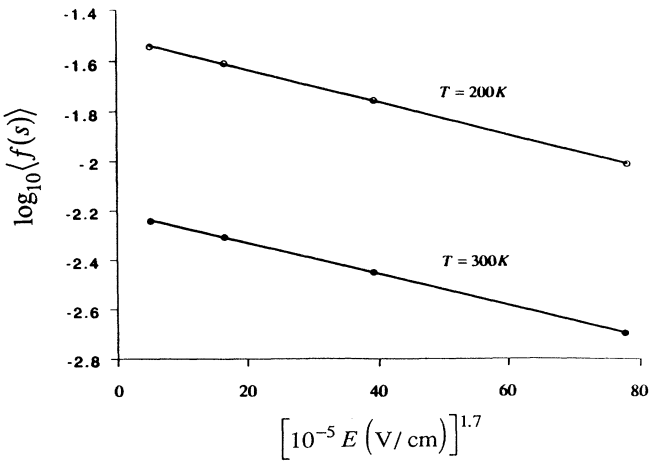

FIG. 8. For $s/\nu_0=10^{-3}$, the $\log_{10}\langle f\rangle$ is plotted as a function of $E^{1.7}$, at the temperatures $T=300$ and 200 K, for a Gaussian distribution of site energies. The points were obtained from $\log_{10}\langle f(s)\rangle$ vs $\log_{10}(s/\nu_0)$ curves for four values of the electric field. These lie on straight lines when plotted versus the electric field raised to a power $\xi\cong1.7$. The slopes are not functions of temperature, which suggests the empirical relation (5.21) between f and E.

The straight lines in Fig. 8 were obtained from (5.21) for $\xi=1.7$ and $C_3=0.82$. The fact that the lines are parallel for both $T=300$ and 200 K indicates that the parameters C_3 and ξ are independent of temperature, and are therefore functions of only M. The lack of temperature dependence of C_3 and ξ suggests that the field dependence of the distribution of pausing times is primarily determined by the field dependence of the (temperature-independent) distribution $g(\varepsilon)$.

To obtain an approximate analytic expression for the mobility, we have fit a tangent to the $\log_{10}\langle f_{E=0}(s)\rangle$ vs $\log_{10}s$ curve at $s/\nu_0=10^{-3}$; as suggested above, we have replaced the function $\langle f_{E=0}(s)\rangle$ by the power law $\langle f_{E=0}(s)\rangle\cong C_4(s/\nu_0)^{\alpha}$. Substituting (5.21) into (5.19) is equivalent to reducing the length L by the factor $\exp[-C_3(eE\rho/\sigma)^{\xi}]$. If we make the appropriate substitutions in (5.11), i.e., substitute $L\exp[-C_3(eE\rho/\sigma)^{\xi}]$ for L, and C_4 for $\Gamma(1-\alpha)$, and solve for the mobility, we obtain

$$\mu=\nu_0\frac{L}{E}\left[\frac{\rho C_1\tanh[C_2(eE\rho/\sigma)]\exp[C_3(eE\rho/\sigma)^{\xi}]}{LC_4\Gamma(1+\alpha)}\right]^{1/\alpha}. \tag{5.22}$$

For small C_2, we have

$$\ln\mu=\left[\frac{1}{\alpha}-1\right]\ln(eE\rho/\sigma)+\frac{C_3}{\alpha}(eE\rho/\sigma)^{\xi}+\left[\ln(\nu_0eL\rho/\sigma)+\frac{1}{\alpha}\ln\left[\frac{\rho C_1C_2}{LC_4\Gamma(1+\alpha)}\right]\right]. \tag{5.23}$$

The field dependence observed in experiment is described well by the first two terms in (5.23). At low fields $\log\mu$ scales with $\log E$, and increases with field with the proportionality factor $1/\alpha-1$, as described by (5.13). However, when $\log E$ is plotted versus $\sqrt{E}$ it is soon apparent that this functional form alone deviates substantially from a straight line, becoming flatter at high fields as $\log E$ ceases to keep up with $\sqrt{E}$. In contrast to the case of a uniform distribution, the exponential factor $\exp[C_3(eE\rho/\sigma)^{\xi}]$ in (5.22) becomes active at high fields and continues the increase of the mobility with field which was begun by the logarithmic term at low fields.

For a uniform distribution of site energies, we argued that α should be proportional to the coordination number M and inversely proportional to βW [cf. Eq. (5.8)]. For the Gaussian distribution of site energies, we have taken an effective α to be the slope of the $\log\langle f(s)\rangle$ vs $\log s$ curve at $s/\nu_0=10^{-3}$. We find similar behavior in that there is good agreement with the empirical expression

$$\alpha=\frac{\alpha_0}{\beta\sigma}\ , \tag{5.24}$$

where $\alpha_0=\alpha_0(M)$. For $s/\nu_0=10^{-3}$ and $M=12$, $\alpha_0=2.34$. Because α is inversely proportional to $\beta\sigma$, the slope of $\log\mu$ versus E increases as temperature decreases, a tendency which is in agreement with the experimental

data. The parameter C_4 in (5.22) depends on the coordination number and the temperature. For $M=12$ we find that $C_4 \cong 3.9\exp(-0.23\beta\sigma)$.

In Fig. 9 we have graphed the log of the mobility, as expressed by (5.22), as a function of $\sqrt{E}$, for the temperatures $T=200$, 230, 260, 290, 320, and 350 K. We have taken the values for the five input parameters as follows: $M=12$, $\sigma=0.10$ eV, $\rho=9$ Å, $\nu_0=10^{13}$ s^{-1}, and $L=1000\rho$. As discussed above, we have used the slope and intercept of the $\log_{10}\langle f(s)\rangle$ vs $\log_{10}s$ curves at $s/\nu_0=10^{-3}$ to obtain the parameters $\alpha_0=2.34$, $C_4=3.9\exp(-0.23\beta\sigma)$, $C_3=0.82$, and $\xi=1.7$. In passing, we note from (5.24) that at $T=300$ K, $\alpha=0.6$, which is indicative of highly dispersive transport. For $M=12$, the parameters C_1 and C_2 describing $l_1(E)$ were found above to be 0.50 and 1.00, respectively. The theoretical curves, which are indicated on the graph by points, are s-shaped, in the direction of deviations from the straight line fits which have been observed by Scott, Pautmeier, and Schein.[5] The $\log(E)$ plunges steeply as E goes to zero, producing a substantial deviation from the observed $\sqrt{E}$ dependence in the low-field regime. For intermediate fields, however, the theory is in reasonable agreement with the $\sqrt{E}$. The straight lines through the points were all generated by the same expression,

$$\log_{10}(\mu)=\log_{10}(e)\times\left[-\frac{\Delta}{kT}+B\left[\frac{1}{kT}-\frac{1}{kT_0}\right]\sqrt{E}+\text{const}\right], \tag{5.25}$$

where const$=8.3$ for μ in cm^2/V s, and $\Delta=0.45$ eV, $B=1.9\times10^{-4}$ $(e^2\,\text{V cm})^{1/2}$, and $T_0=600$ K. Thus our result is in agreement with the form proposed by Gill, and the magnitude of the quantities Δ, B, and T_0 are typical of experiment. It is interesting that the *apparent* zero-field activation energy, Δ, is almost a half an electron volt, while the standard deviation of the Gaussian density of states is only 0.1 eV. We should point out that the agreement of our result with the $\sqrt{E}$ is relatively insensitive to the values of many of the parameters. Although we have found the exponent, $\xi=1.7$, the coincidence of (5.22) with $\sqrt{E}$ is as good for ξ anywhere between 1 and 2. Also, l_1 may as well be linear in E; the saturation of the hyperbolic tangent does not affect the result except at high fields, and then the first term in (5.23) is no longer important.

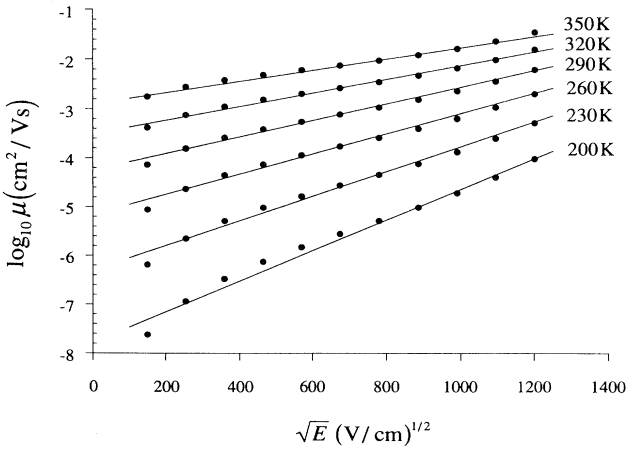

FIG. 9. The $\log_{10}\mu$ is shown as a function of the $\sqrt{E}$ for temperatures from 200 to 350 K. The points are calculated from (5.22). The input parameters are $M=12$, $\sigma=0.1$ eV, $L/\rho=1000$, $\rho=9$ Å, and $\nu_0=10^{13}$ s^{-1}. The calculated parameters are $C_1=0.50$, $C_2=1.00$, $C_3=0.82$, $C_4=3.9\exp(-0.23\beta\sigma)$, $\xi=1.7$, and $\alpha_0=2.34$. The straight lines are generated from the Gill form for the exponential dependence, as expressed in (5.25), with $\Delta=0.45$ eV, $B=1.9\times10^{-4}$ $(e^2\,\text{V cm})^{1/2}$, and $T_0=600$ K.

The range of electric field spanned in Fig. 9 is the range for which the theory most closely predicts a linear dependence of $\log\mu$ on $\sqrt{E}$. At higher fields the theory predicts that $\log\mu$ should increase as E^{ξ}; for $\xi=1.7$, our results begin to deviate significantly from the $\sqrt{E}$ law when $E>1.5\times10^6$ V/cm. For $E<4\times10^4$ V/cm, on the other hand, the mobility predicted by (5.22) begins to decrease much faster than the $\sqrt{E}$ law, approaching zero as the field goes to zero. This is due to the SM component of the theory. When the field is reduced, the number of times the distribution of pausing times is sampled increases. Adding up all of these times to calculate the total transit time is analogous to summing a divergent series; the total transit time scales faster than the total number of hops n, leading to a mobility which vanishes as $n\to\infty$.

Although the pausing-time distributions calculated in this article appear to decay algebraically at short times, with $\alpha<1$ (cf. Figs. 4 and 7), they are, in fact, exponentially bounded at long times. Consequently, as $n\to\infty$, the *effective* disorder parameter α tends to one, and the zero-field mobility approaches a nonvanishing value which is independent of field. Further analysis of the time dependence of the effective α is required to quantitatively characterize this low-field behavior. Nevertheless, if the pausing-time distribution associated with a particular sample decays algebraically for long enough times, it may appear that the low-field mobility approaches zero, in agreement with (5.22). Experimental data for the hole transport in tri-*p*-tolylamine-doped bisphenol-A-polycarbonate (TPA) shows this tendency at low fields.[17]

VI. DISCUSSION

As discussed in the Introduction, one objection to the results expressed by (5.12) and (5.22), and in fact to the application of the Scher-Montroll theory in general, is that the anomalous features which were explained by SM, and which are seen in the amorphous semiconductors, are no longer seen in recent experiments on the molecularly doped polymers. In most experiments the shoulder of the current-time curves is clearly visible on a linear scale, and the current is essentially a constant as a function of time.[32,33] In addition, the theory of Scher and Montroll predicts that the measured mobility should scale with the length of the sample, when in fact it is

found to be *independent* of thickness.[17] On the other hand, there are still some experimental signatures of anomalous transport remaining. For example, after the shoulder, the decay of the current indicates that the carrier packet is still very broad, with the width w of the packet clearly scaling as the transit time τ rather than the $\sqrt{\tau}$, as one might expect for normal Gaussian transport.[33,34] Furthermore, the current-time curves continue to show universality.[33] It is indeed puzzling that, in spite of all these differences in experimental features, the field dependence of the mobility has remained the same. That is, the field dependence for most experiments continues to be described well by (5.23). We speculate below on a simple answer to this puzzle. First we remind the reader of a well-known inconsistency in applying the SM theory to a problem with static disorder.

The n-fold convolutions of the pausing-time distribution which enter into expression (4.4) indicate that the time to make n hops should be found by drawing n-independent times from the distribution and adding them together. However, if the distribution of dwell times is the result of static disorder, the procedure of adding the times should strictly apply to transport in one spatial dimension, and even then, to the case in which none of the old sites is revisited.[35] For higher dimensions, there should be a tendency to characterize transport by an addition of rates rather than an addition of times since, in higher dimensions, the current may choose between many parallel avenues. One wonders, in fact, why the anomalous scaling of SM should be observed at all in a three-dimensional system. It is possible, however,that the procedure of adding times may be approximately correct for systems of this type when the transport process is looked at from the point of view of percolation theory.

When the hopping rates become extremely disparate as a result of spatial and energetic disorder, it is widely recognized that only a few of the many available paths will be of relevance to transport. According to Ambegoakar, Halperin, and Langer[36] such systems are to be characterized as nearly percolating; conduction occurs predominantly through that subnetwork of the most well-connected sites below which a connected path fails to exist. We know from percolation theory that about 25% of the bonds must be intact to form a connected path in three dimensions. Since in a real system no bonds are truly broken, the conductivity is actually that of a network which is slightly more connected than that of a true percolating cluster at threshold. Thus, there will be a length scale $\mathcal{L}$ above which the system may be again viewed as a three-dimensional network, each bond of which is associated with a percolating substructure with spectral dimension $1<d<2$.[37] This suggests that if the SM theory, which is based on adding the dwell times, is to apply to a system with static disorder, it is to the crossover length scale $\mathcal{L}$ below which transport is of lower effective dimensionality. At longer lengths the anomalous transport of SM should cease. We should see length-dependent scaling of the mobility only if the thickness of the sample L is smaller than the typical length of a connecting pathway $\mathcal{L}$. If $L \gg \mathcal{L}$, equation (5.11) should not give the time τ to traverse the sample. Instead, it should give the time $\tau_{\mathcal{L}}$ to traverse a connect of length $\mathcal{L}$;

$$\tau_{\mathcal{L}}=\frac{1}{\nu_0}\left[\frac{\mathcal{L}}{l_1}\Gamma(1-\alpha)\Gamma(1+\alpha)\right]^{1/\alpha} . \tag{6.1}$$

If L is some multiple $\mathcal{M}$ of the length $\mathcal{L}$, then the time τ to traverse the sample should scale as $\mathcal{M}\tau_{\mathcal{L}}$. In this way, the mobility,

$$\mu=\frac{L}{\tau E}=\frac{\mathcal{M}\mathcal{L}}{\mathcal{M}\tau_{\mathcal{L}}E}=\frac{\mathcal{L}}{\tau_{\mathcal{L}}E} , \tag{6.2}$$

becomes an intrinsic property of the sample. Yet it still retains *exactly* the same field dependence. On a larger scale, each connect should be viewed as a *field-directed* bond across which may be defined a macroscopic (field-dependent) jump rate $F \propto 1/\tau_{\mathcal{L}}$. The qualitative effects of such an intrinsic length on the current-time curves are in keeping with experiment; after a time $\tau_{\mathcal{L}}$ the current-time curve should begin to level off, and normal transport should resume, since the full three dimensionality of the sample should be felt. However, if the width of the carrier packet increases by an amount h while traversing each connect, then after the packet has traversed $\mathcal{M}$ connects its width should be proportional to $h\sqrt{\mathcal{M}}$. From SM universality, h should be proportional to $\tau_{\mathcal{L}}$. Therefore, after the carrier packet traverses the entire sample, its width w should scale with the transit time and sample length as

$$w \propto \tau_{\mathcal{L}}\sqrt{\mathcal{M}} \propto \frac{\tau}{\sqrt{L}} . \tag{6.3}$$

That is, if there is an anomalous spreading of the carrier packet in traversing each connect, there should also be an anomalous scaling of w at longer length scales.

As we have already mentioned, the transport formalism developed here in the absence of topological memory does not account for parallel paths, and thus leads to the SM result which suggests quasi-one-dimensional (1D) transport. To correctly weight the various paths to obtain an effective distribution of pausing times one should obtain corrections to the self-energy in an expansion for the Green function of the master equation. In practice, however, accounting for all paths is difficult.[38,39] To partially correct the present approach we should attempt to account for the fact that some sites may be visited more than once. That is, we should not draw *n-independent* times from the distribution of pausing times to evaluate the time it takes a random walker to make n hops, for many of these times should be repeats. The simplest case in which such overlap may be characterized is for a 1D chain aligned in the direction of the electric field. It is clear that the average number of times K that a site will be revisited must be inversely proportional to E, that is, $K \propto 1/E$. In higher dimensions, K may be estimated from the solution of the master equation (on an ordered lattice) in the presence of a bias. The average number of times a site will be revisited is proportional to the infinite time integral of the probability to remain at the origin. For the dimensionality $d>2$, K is a constant, indepen-

dent of the electric field. However, for $1<d<2$, K scales with the field. One finds that

$$K_d \propto \frac{1}{E^{2-d}} . \tag{6.4}$$

To correct (4.4) with (6.4) we note that, in (4.4), $\tilde{\psi}_n(s)$ should no longer be given by $\tilde{\psi}(s)^n$, but given instead by $\tilde{\psi}(K_d s)^{n/K_d}$, where n/K_d is the number of *unique* dwell times sampled, and $\tilde{\psi}(K_d s)$ is the Laplace transform of the distribution of times which has been broadened by the scale factor K_d. Carrying through the algebra to (5.13), we find that

$$\ln\mu \propto (d-1)(1/\alpha-1)\ln E . \tag{6.5}$$

For low dimensions, the rate at which the mobility increases with field is diminished. To understand this tendency we note that there is a price which is paid for successful motion, and that is the opportunity to sample new dwell times which might be extraordinarily long. This cost is a stronger function of field as the dimensionality is reduced. It is interesting that in the one dimension ($d=1$) for which the addition of dwell times (to determine the mobility) is clearly appropriate, the dependence of the mobility on the electric field vanishes.

In writing our main result, expression (5.22), we have characterized the mobility by a disorder parameter α which is less than 1, in spite of the fact that strict algebraic scaling of the SM type is not found in the model; for the case of a Gaussian distribution of site energies, it can be shown from (5.20) that, as $s\to 0, \langle f(s)\rangle \sim s$, rather than s^α, which would be the case for anomalous transport. On plotting $\langle f(s)\rangle$ versus s, however, we note (cf. Fig. 7) that when $\langle f(s)\rangle$ is described by the function $s^{\alpha(s)}$, the exponent $\alpha(s)$ varies slowly, from $\alpha\cong 0.4$ at $s/\nu_0=10^{-1}$, to $\alpha\cong 0.8$ at $s/\nu_0=10^{-5}$. This means that if the time of interest is not too long, the mobility may be appropriately characterized by an *effective* disorder parameter after all. Since ν_0 is the upper limit on the hopping rate, we suggest, for example, that the effective value of α for random walks which average only ten hops will be greater than 0.4, whereas for random walks consisting of 10^5 hops the effective α will be greater than 0.8. This behavior is not surprising. In fact, the implications to the current-time curves of such a "time-dependent α" have been investigated previously,[40] and crossovers from dispersive to nondispersive transport as a function of sample length and electric field have been discussed.[41] In none of these investigations, however, have considerations been given to an intrinsic length $\mathcal{L}$, or to a site-return parameter K. Further study is needed in this direction, therefore, in order to sharpen the concept of an effective disorder parameter.

The rationale for examining the Miller-Abrahams form of the hopping rate, and for choosing a Gaussian density of states with $\sigma=0.1$ eV, was to establish contact with the Monte Carlo simulations of Bässler.[21] As discussed in the Introduction, simulation results are in agreement with many aspects of experiment. Our approach has been to follow the implementation of a computer simulation as closely as possible, and to introduce approximations when needed to maintain some degree of analyticity. In this manner we have sought to improve upon the disorder-based explanations for the behaviors observed in both simulation and experiment. Indeed, one of the primary contributions of this article is to offer an explanation for a strong increase of mobility with E at high fields when the hopping rates are of the Miller-Abrahams type. We have found additional agreement with experiment, however, which goes beyond agreement with simulation; our analysis gives rise to an increase of the mobility with $\sqrt{E}$ for the range 2×10^4 V/cm $<E<1.5\times 10^6$ V/cm, whereas simulations do not show good agreement with an increasing $\sqrt{E}$ law until $E>10^5$ V/cm. Although a variety of approximations necessarily distinguish our results from the exact results of Monte Carlo simulations, the difference in predicted behavior suggests that the Monte Carlo simulations lack the mechanism for the first of the two field-dependent terms in (5.23), $(1/\alpha-1)\ln(eE\rho/\sigma)$. This term, which provides for an increase of mobility with field for small fields, is intimately tied to anomalous dispersion. In the present analysis we have retained this effect at small fields by choosing an effective dispersion parameter α from the slope of the $\log\langle f\rangle$ vs $\log s$ curve at the arbitrary fixed value $s=10^{-3}\nu_0$. As we have remarked above, however, we should instead choose α self-consistently, from the slope of the $\log\langle f\rangle$ vs $\log s$ curve at $s\approx 1/\tau$, where τ is the transit time (which depends on α). The correction this brings to (5.23) is a field dependence to the dispersion parameter, such that α *decreases* with increasing E. There is then an additional field-dependent term in (5.23); the negative term,

$$\frac{1}{\alpha}\ln\left[\frac{\rho C_1 C_2}{L C_4 \Gamma(1+\alpha)}\right] ,$$

becomes more negative as α decreases. For the present study, α varies slowly with E, and the corrections to the results shown in Fig. 9 are small over the field range 2×10^4 V/cm $<E<1.5\times 10^6$ V/cm (assuming $\mathcal{L}=1000\rho$). If more degrees of freedom are included, however, the variation of α with E becomes stronger. Were we, for example, to consider spatial fluctuations in r in addition to the variations in θ and ε_2, the multidimensional Poissonian distribution of nearest-neighbor hyperradii would decay more rapidly with $\mathcal{R}$. As a result, the corresponding pausing-time distribution would decrease more rapidly with t, giving rise to a stronger time dependence to the effective disorder parameter α, which implies a stronger field dependence. If the rate at which α decreases with E were fast enough, the decrease of the third term in (5.23) with E would begin to counter the increase of the first two terms with E. Consequently, the low-field mobility would increase less quickly with increasing E, which is the tendency observed in Monte Carlo simulations. For this reason we expect that the results of the present analysis will show better agreement with the results of Monte Carlo simulations when the analysis is extended to include spatial fluctuations in r. Conversely, the results of Monte Carlo simulations might be in closer agreement with the experimental $\sqrt{E}$ law at low

fields if the number of independent means by which disorder is introduced in the model (degrees of freedom) is reduced.

We have not addressed the concentration dependencies and other effects related to spatial disorder. Our purpose is to explain the $\sqrt{E}$ with as simple a disorder theory as possible, and to focus on the reported temperature dependence of the Poole-Frenkel factor and the dispersion parameter α. It is known that the inclusion of spatial disorder generally introduces a time-dependent α, in the sense that $\psi(t)$ as given by (5.7) decays as $1/t^{1+c\ln^2(t)}$ at long times. Combined with energetic disorder from a power-law density of states which begins at $\varepsilon=0$ and increases as ε^{ν}, one can show that $\psi(t)\sim 1/t^{1+c\ln^{3+\nu}(t)}$. Including spatial disorder, therefore, compels one to examine more carefully the consequences of a time-dependent effective α, in order to extract appropriate field and concentration dependencies.[35] Nevertheless, we can infer *some* information about the concentration dependence of B and T_0 in our simple calculations if we assume that the primary effect of decreasing the concentration of dopants is to reduce the coordination number M. From (5.9) and (5.17) we see that a reduction of concentration should lower α and increase B, assuming that W remains constant. This tendency is in agreement with experiment. However, we see also from (5.18) that a decrease in concentration should increase T_0. This is in contrast to the experimental results which show generally a decrease in T_0 as the mean dopant spacing becomes larger.[8]

One of the most intriguing aspects of the theory is the determination of an effective activation energy, Δ, which is inferred from (5.23) by fitting $\ln\mu$ versus $\sqrt{E}$ to straight lines in the field range of interest, and then extrapolating these lines to zero field. From the straight-line fits of the curves in Fig. 9, we find that $\Delta\cong 0.5$ eV, which is rather large considering that σ is only 0.1 eV. The temperature dependence of the mobility is, however, determined by the parameter α, and therefore the effective activation energy is determined by the input parameters ρ, $\mathcal{L}$, σ, and M, the derived parameters C_1, C_2, C_3, C_4, and ξ, as well as the strength of the electric field in midrange, E_0. Hence the relationship between σ and Δ is not as direct as one is led to from the analytic form of the underlying hopping rate. This observation has considerable bearing on recent discussion regarding the nature of hopping in these systems[42]—whether it is polaronic, in which case the activation energy would arise in part from lattice distortions which accompany the moving of charge, or whether it is of the Miller-Abrahams form, in which case it would be entirely due to static disorder, or whether it is some combination of each. Here we see, for example, that an apparent activation energy of $\Delta\cong 0.5$ eV is not incompatible with a model in which the Miller-Abrahams form of the jump rate is assumed, although further predictions of the concentration dependence of Δ will require a more complete analysis which includes variations in r. In a recent study of small-polaron hopping in an energetically disordered environment in which variable-range hopping techniques were applied, it was suggested that the increase in Δ as a function of concentration in TPD-doped polycarbonate arises as a result of selection of the most favorable conducting path.[43] While this may indeed be the case, that analysis suffers from the fact that the results depend on an arbitrarily chosen initial energy ε_1, rather than on the self-consistent distribution $g(\varepsilon)$. In addition, the analysis was carried out in the linear regime, which is inappropriate if the apparent activation energy in these systems is largely an artifact of the extrapolation of linear fits to the $\sqrt{E}$. It will be instructive, therefore, to reexamine the applicability of a disorder model in which the underlying hopping rate is polaronic, in the context of the present theory.

VII. SUMMARY

In this article we began with a description of a continuous time random walk in a disordered material, and from this, developed a theory which recovers the key features of anomalous transport. In developing analytic expressions, we began with the formulation of variable-range hopping as presented by Apsley and Hughes and used the distribution of nearest-neighbor hyperradii to calculate a distribution of dwell times and a distribution of hopping distances. For tractability, these calculations were carried out under the assumption that after each step in the random walk all topological memory is lost. We focused on energetic disorder, and included the aspects of spatial disorder only in the sense that the nearest-neighbor sites may be distributed at random points on a sphere of constant radius. The difficulty in addressing energetic disorder is that the hopping rates in general depend on both the energy of the final site and energy of the initial site. Whereas the distribution of final site energies is known, or at least postulated *a priori*, the distribution of energies of the initial sites depends on the history of the random walk. We obtained the distribution of initial energies by applying the self-consistency condition (3.9). In addressing the experiments in the molecularly doped polymers, we considered a Miller and Abrahams form for the underlying hopping rate. For the case of a Gaussian distribution of site energies, we obtained an expression for the mobility which closely follows a straight line as a function of $\sqrt{E}$. The temperature dependence of the logarithmic slope follows the Gill form of the Poole-Frenkel factor, having both Arrhenius and compensation terms.

ACKNOWLEDGMENTS

The author is grateful to many who have assisted with this article: to Paul Parris and Nitant Kenkre, for discussions on the mechanism of transport; to John Andersen, for conversations on percolation theory, and for his invaluable contributions in the preparation of the manuscript; to Larry Schein, Campbell Scott, Paul Borsenberger, and Ralph Young, for their patience in explaining the subtleties of transport in molecularly doped polymers; and to Byron Dieterle, for the use of the DEC Alpha 3000/400 workstation. The self-consistency equation (3.9) was developed in collaboration with Paul Parris, and Gary Herling is to be thanked for his insight regarding its solution.

[1]D. M. Pai, J. Chem. Phys. **52**, 2285 (1970).
[2]J. Frenkel, Phys. Rev. **54**, 647 (1938).
[3]The number of experimental results is too large to cite each individually. For a comprehensive list and discussion, see, P. M. Borsenberger and D. S. Weiss, *Organic Photoreceptors for Imaging Systems* (Dekker, New York, 1993), Chap. 8, p. 181, or one of the many review articles referenced therein.
[4]W. D. Gill, J. Appl. Phys. **43**, 5033 (1972).
[5]J. C. Scott, L. Th. Pautmeier, and L. B. Schein, Phys. Rev. B **46**, 8603 (1992).
[6]P. M. Borsenberger, L. Pautmeier, and H. Bässler, J. Chem. Phys. **94**, 5447 (1991).
[7]L. B. Schein, A. Peled, and D. Glatz, J. Appl. Phys. **66**, 686 (1989).
[8]J. X. Mack, L. B. Schein, and A. Peled, Phys. Rev. B **39**, 7500 (1989).
[9]G. Pfister, Phys. Rev. B **16**, 3676 (1977).
[10]G. Pfister and H. Scher, Adv. Phys. **27**, 747 (1978).
[11]J. Hirsch, J. Phys. C **12**, 321 (1979).
[12]M. Stolka, J. F. Yanus, and D. M. Pai, J. Phys. Chem. **88**, 4704 (1984).
[13]H. Scher and E. W. Montroll, Phys. Rev. B **12**, 2455 (1975).
[14]N. Crisa, Phys. Status Solidi B **116**, 269 (1983).
[15]P. M. Borsenberger, W. Mey, and A. Chowdry, J. Appl. Phys. **49**, 273 (1978).
[16]P. M. Borsenberger, R. Richert, and H. Bässler, Phys. Rev. B **47**, 4289 (1993).
[17]P. M. Borsenberger, J. Appl. Phys. **68**, 6263 (1990).
[18]H. Bässler, Philos. Mag. **50**, 347 (1984).
[19]L. Pautmeier, R. Richert, and H. Bässler, Philos Mag. Lett. **59**, 325 (1990); Philos. Mag. B **63**, 587 (1991).
[20]R. Richert, L. Pautmeier, and H. Bässler, Phys. Rev. Lett. **63**, 547 (1989).
[21]H. Bässler, Int. J. Mod. Phys. B **8**, 847 (1994); H. Bässler, Phys. Status Solidi B **175**, 15 (1993).
[22]M. Grunewald, B. Pohlmann, B. Movaghar, and D. Wurtz, Philos. Mag. **49**, 341 (1984).
[23]B. Movaghar, M. Grunewald, B. Ries, H. Bässler, and D. Würtz, Phys. Rev. B **33**, 5532 (1986).
[24]A. Yelon and B. Movaghar, Phys. Rev. Lett. **65**, 618 (1990).
[25]B. Movaghar, A. Yelon, and M. Meunier, Chem. Phys. **146**, 389 (1990).
[26]N. Apsley and H. P. Hughes, Philos. Mag. **30**, 963 (1974).
[27]A. Miller and E. Abrahams, Phys. Rev. **120**, 745 (1960).
[28]D. Emin, Adv. Phys. **24**, 305 (1975).
[29]V. M. Kenkre and D. H. Dunlap, Philos. Mag. B **65**, 831 (1992).
[30]N. F. Mott, Philos. Mag. **19**, 835 (1969).
[31]R. G. Kepler, Phys. Rev. **119**, 1226 (1960); O. H. LeBlanc, J. Chem. Phys. **32**, 626 (1960).
[32]M. Abkowitz, M. J. Rice, and M. Stolka, Philos. Mag. B **61**, 25 (1990).
[33]L. B. Schein, J. C. Scott, L. Th. Pautmeier, and R. Young, Mol. Cryst. Liq. Cryst. **228**, 175 (1992).
[34]P. M. Borsenberger and H. Bässler, J. Appl. Phys. **75**, 967 (1994).
[35]H. Schnoerer, D. Haarer, and A. Blumen, Phys. Rev. B **38**, 8097 (1988).
[36]V. Ambegaokar, B. I. Halperin, and J. S. Langer, Phys. Rev. B **4**, 2612 (1971).
[37]M. B. Isichenko, Rev. Mod. Phys. **64**, 961 (1992).
[38]C. R. Gochanour, H. C. Andersen, and M. D. Fayer, J. Chem. Phys. **70**, 4245 (1979).
[39]J. Klafter and R. Silbey, J. Chem. Phys. **72**, 843 (1980); A. Blumen, J. Klafter, and R. Silbey, *ibid.* **72**, 5320 (1980).
[40]J. Noolandi, Phys. Rev. B **16**, 4466 (1977).
[41]E. Muller-Horsche and D. Haarer, Phys. Rev. B **35**, 1273 (1987).
[42]L. B. Schein, Philos. Mag. B **65**, 795 (1992).
[43]D. H. Dunlap and V. M. Kenkre, Chem. Phys. **178**, 67 (1993).